Journal of Alloys and Compounds 509 (2011) 457–462

Contents lists available at ScienceDirect

Journal of Alloys and Compounds

journal homepage: www.elsevier.com/locate/jallcom

Spectroscopic and photoluminescence properties of Dy^{3+}-doped lead tungsten tellurite glasses for laser materials

A. Mohan Babu [a], B.C. Jamalaiah [b], J. Suresh Kumar [a], T. Sasikala [a], L. Rama Moorthy [a,*]

[a] Department of Physics, Sri Venkateswara University, Tirupati, 517 502, India
[b] Department of Physics, Pukyong National University, Busan, 608 737, Republic of Korea

ARTICLE INFO

Article history:
Received 17 June 2010
Received in revised form 7 September 2010
Accepted 8 September 2010
Available online 22 September 2010

Keywords:
Amorphous materials
Solid state reactions
Optical properties
Luminescence

ABSTRACT

Lead tungsten tellurite (LTT) glasses doped with different Dy^{3+} ion concentrations have been prepared and characterized through optical absorption, photoluminescence and decay measurements. The glassy nature of the LTT host has been confirmed through the XRD measurements. The three phenomelogical intensity parameters Ω_λ ($\lambda = 2, 4, 6$) have been determined from the absorption spectral intensities using the Judd–Ofelt (J–O) theory. The hypersensitivity of $^6H_{15/2} \rightarrow {}^6F_{11/2}$ transition based on the magnitude of Ω_2 parameter has also been discussed. By using the J–O intensity parameters several radiative properties such as spontaneous transition probabilities (A_R), fluorescence branching ratios (β_R) and radiative lifetimes (τ_R) have been determined. The effect of Dy^{3+} ion concentration on the emission intensities of $^4F_{9/2} \rightarrow {}^6H_{J'}$ ($J' = 15/2$, 13/2, 11/2 and 9/2) transitions has also been reported.

1. Introduction

Several glass matrices such as fluorides, phosphates, borates, fluorophosphates, fluoroborates, fluorozirconates, sulfides, selenides and tellurites have been widely investigated to understand the effect of the host on the lasing properties of the rare-earth ions [1–11]. Recently, photoluminescence properties of tellurite and heavy metal oxide glasses doped with rare earth ions have been studied due to their low phonon energies, high refractive indices and good rare-earth ions solubility [12]. In general, host glasses with low phonon energies provide less non-radiative relaxation rates and high fluorescence quantum efficiencies. Tungsten based materials are well known for their electro-chromic and photo-chromic properties as well as their wide range of practical applications in smart windows, display devices and sensors [13–15]. Moreover, the addition of lead fluoride (PbF_2) decreases the host phonon energy and thereby suppresses the non-radiative losses.

The knowledge on transition probabilities of 4f–4f transitions of rare-earth ions is very important for the characterization of laser glasses. Among trivalent lanthanides, the Dy^{3+} ions doped into several glasses and crystals have been investigated in order to obtain two primary color (yellow or blue) luminescent materials because of its yellow emission at 570–600 nm corresponding to the $^4F_{9/2} \rightarrow {}^6H_{13/2}$ hypersensitive transition and the blue emission at 470–500 nm corresponding to the $^4F_{9/2} \rightarrow {}^6H_{15/2}$ transition. Thus, the yellow-to-blue (Y/B) luminescence intensity ratio can be modulated by varying the host glass, Dy^{3+} concentration, its chemical composition, excitation wavelengths and heat treatment for the generation of white light [9].

In order to investigate the characteristic visible emission of Dy^{3+} ions due to $^4F_{9/2} \rightarrow {}^6H_J$ ($J = 15/2$, 13/2, 11/2 and 9/2) transitions, the authors selected the tellurite based TeO_2–WO_3–PbF_2 host composition. The present work reports the spectroscopic investigations of LTT glasses doped with different concentrations of Dy^{3+} ions and their luminescence characteristics for the generation of intense blue (484 nm) and yellow (586 nm) emissions.

2. Experimental techniques

Glasses with the molar composition (in mol%) of $15PbF_2 + 25WO_3 + (60 - x)TeO_2 + xDy_2O_3$ (where $x = 0.1$, 0.5, 1.0 and 2.0) were prepared by the melt quenching technique and they were referred as LTTDy01, LTTDy05, LTTDy10 and LTTDy20 glasses, respectively. The starting chemicals of TeO_2, WO_3, PbF_2 and Dy_2O_3 were mixed in an agate mortar to get homogeneous mixture and then melted in a platinum crucible at 700–750 °C for 40 min in an electrical furnace. The melt was poured on to a preheated brass mould and annealed at 300 °C for 12 h to remove thermal strains and then allowed to cool to room temperature.

The glassy nature of the samples was confirmed by XRD pattern using Siefert X-ray diffractometer with CuKα as the radiation source at 40 kV and 30 mA. The densities were measured according to the Archimedean's principle using xylene as immersion liquid. For refractive index measurements, the Brewster's angle method has been adopted using a 2 mW He–Ne polarized laser (632.9 nm) as light source. For LTTDy10 glass, the measured density and refractive index values are 6.569 g/cm^3 and 2.2326, respectively. The absorption spectrum has been recorded using Varian Cary 5E UV–vis–NIR spectrophotometer in the range of 700–2100 nm. The excitation ($\lambda_{em} = 576$ nm), photoluminescence ($\lambda_{ex} = 452$ nm) and decay ($\lambda_{em} = 576$ nm

* Corresponding author. Tel.: +91 877 2289472; fax: +91 877 222521.
E-mail address: lrmphysics@yahoo.co.in (L.R. Moorthy).

0925-8388/$ – see front matter © 2010 Elsevier B.V. All rights reserved.
doi:10.1016/j.jallcom.2010.09.058

and λ_{ex} = 452 nm) measurements were carried out using JOBIN YVON Fluorolog-3 spectrofluorimeter with xenon flash lamp as light source.

3. Theory

The absorption spectra of lanthanides arise due to intraconfigurational f–f transitions. The majority of transitions are induced electric dipole in nature. The intensities of the absorption bands can be expressed in terms of measured oscillator strengths (f_{meas}) by the area method using the formula [16]

$$f_{meas} = 4.32 \times 10^{-9} \int \varepsilon(\nu)\, d\nu \quad (1)$$

where $\varepsilon(\nu)$ is the molar absorptivity at energy ν (cm^{-1}) and can be obtained using Beer–Lambert's law. The Judd–Ofelt (J–O) model [17,18] gives the theoretical estimation of the intensities of intraconfigurational f–f transitions of lanthanide ions. According to this model, the transition intensities are characterized by the three phenomenological parameters Ω_λ (λ = 2, 4, 6) known as J–O intensity parameters, which depend on the local environment. The calculated oscillator strengths (f_{cal}) of the transitions from the initial state ψJ to the final states $\psi' J'$ are given by

$$f_{cal}(\psi J, \psi' J') = \frac{8\pi mc\nu}{3h(2J+1)} \left[\frac{(n^2+2)^2}{9n} S_{ed}(\psi J, \psi' J') + n S_{md}(\psi J, \psi' J') \right] \quad (2)$$

where m is the electron mass, c is the speed of light, h is the Plank's constant ($2J+1$) is the degeneracy of the ground state. The factor $(n^2+2)^2/9n$ is the Lorentz local field correction factor which indicates that the Dy^{3+} ion is not in vacuum but in a dielectric medium of refractive index n. The S_{ed} and S_{md} are the electric and magnetic dipole linestrengths, respectively. The evaluated set of J–O intensity parameters obtained by the least square fit can be used to determine several radiative properties of lanthanide ions. The spontaneous emission probabilities from the excited level ψJ to the lower lying levels $\psi' J'$ are given by

$$A_R(\psi J, \psi' J') = \frac{64\pi^4 \nu^3}{3h(2J+1)} \left[\frac{n(n^2+2)^2}{9} S_{ed}(\psi J, \psi' J') + n^3 S_{md}(\psi J, \psi' J') \right] \quad (3)$$

The radiative lifetime (τ_R) of an excited state, the luminescence branching ratios (β_R) for different emissions from the same initial level and the stimulated emission cross-sections (σ_e) can be calculated using the equations

$$\tau_R(\psi J) = \frac{1}{\sum_{\psi' J'} A_R(\psi J, \psi' J')} \quad (4)$$

$$\beta_R(\psi J, \psi' J') = \frac{A(\psi J, \psi' J')}{\sum_{\psi' J'} A_R(\psi J, \psi' J')} \quad (5)$$

and

$$\sigma_e(\psi J, \psi' J') = \frac{\lambda_P^4}{8\pi c n^2 \Delta\lambda_P} A_R(\psi J, \psi' J') \quad (6)$$

where λ_p be the peak wavelength and $\Delta\lambda p$ be the effective bandwidth of an emission band.

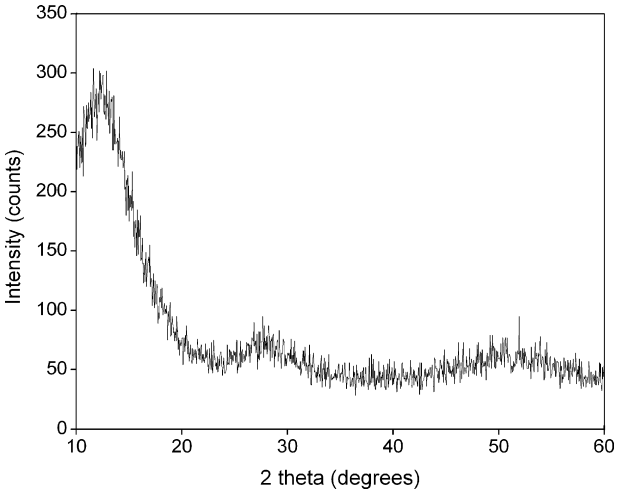

Fig. 1. XRD profiles of LTTDy10 glass.

4. Results and discussion

4.1. Glassy nature

X-ray diffraction studies have been carried out to distinguish the crystalline and non-crystalline nature of LTTDy glasses. XRD measurements show similar patterns for all the samples and the XRD profile of LTTDy10 glass is shown in Fig. 1 for reference. The XRD patterns reveal no distinguishable intensity peaks, but the broad diffusion at low scattering angles indicates the glassy/amorphous nature of the LTT glass system.

4.2. Spectroscopic properties and J–O analysis

Fig. 2 shows the absorption spectrum of LTTDy10 glass recorded at room temperature in the wavelength region 700–2100 nm. Each absorption peak corresponds to the transition from the $^6H_{15/2}$ ground state to various excited states of Dy^{3+} ion. The spectrum consists of six distinct and inhomogeneous broad absorption bands at 753, 802, 905, 1092, 1275 and 1685 nm corresponding to the $^6H_{15/2} \rightarrow {}^6F_{3/2}$, $^6F_{5/2}$, $^6F_{7/2}$, $^6F_{9/2}$, $^6F_{11/2}$ and $^6H_{11/2}$ transitions, respectively. The assignments of the absorption transitions have been done according to Carnall et al. [19] as presented in Table 1.

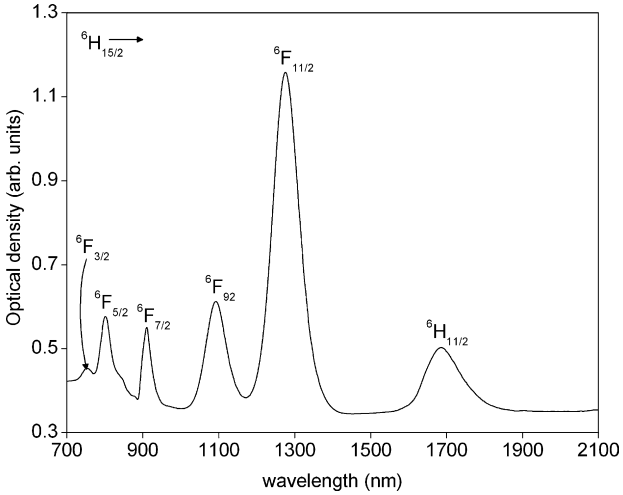

Fig. 2. Room temperature vis–NIR absorption spectrum of LTTDy10 glass.

Table 1
Absorption band positions, measured (f_{meas}) and calculated (f_{cal}) oscillator strengths of LTTDy10 glass.

Transition	Wavelength, λ (nm)	Energy, ν (cm^{-1})	Oscillator strengths ($\times 10^{-6}$)	
			f_{meas}	f_{cal}
$^6H_{15/2} \rightarrow {}^6F_{3/2}$	753	13,280	0.24	0.14
$^6F_{5/2}$	802	12,469	1.31	0.76
$^6F_{7/2}$	905	11,050	1.26	1.86
$^6F_{9/2}$	1092	9158	3.01	2.89
$^6F_{11/2}$	1275	7843	8.92	8.96
$^6H_{11/2}$	1685	5935	0.24	0.14
			$\delta_{rms} = \pm 0.34 \times 10^{-6}$	

Table 2
Comparison of J–O intensity parameters of Dy^{3+} ions in different glasses.

Host lattice	J–O intensity parameters ($\times 10^{-20}$ cm^2)			Trend
	Ω_2	Ω_4	Ω_6	
PbF_2–WO_3–TeO_2 [This work]	5.19	1.93	1.07	$\Omega_2 > \Omega_4 > \Omega_6$
$(NaPO_3)_6$–TeO_2–AlF_3–LiF [21]	7.06	2.20	0.97	$\Omega_2 > \Omega_4 > \Omega_6$
$(NaPO_3)_6$–TeO_2–AlF_3–NaF [21]	5.53	2.13	0.88	$\Omega_2 > \Omega_4 > \Omega_6$
$(NaPO_3)_6$–TeO_2–AlF_3–KF [21]	6.05	2.30	1.09	$\Omega_2 > \Omega_4 > \Omega_6$
ZnO–TeO_3 [22]	4.30	1.32	2.53	$\Omega_2 > \Omega_4 > \Omega_6$
Na_2O–TeO_3 [22]	3.70	1.15	2.22	$\Omega_2 > \Omega_4 > \Omega_6$
BaO–TeO_3 [22]	3.20	1.35	2.47	$\Omega_2 > \Omega_4 > \Omega_6$
PbO–H_3BO_3–TiO_2–AlF_3 [7]	7.05	1.22	1.91	$\Omega_2 > \Omega_4 > \Omega_6$
PbO–B_2O_3–Al_2O_3–WO_3 [23]	4.90	0.94	2.07	$\Omega_2 > \Omega_4 > \Omega_6$

The measured oscillator strengths (f_{meas}) of various observed absorption bands were evaluated using Eq. (1). The Judd–Ofelt analysis has been performed for the measured oscillator strengths by using Eq. (2) in order to obtain the calculated oscillator strengths (f_{cal}) and hence the J–O intensity parameters. Considerably small δ_{rms} deviation of $\pm 0.34 \times 10^{-6}$ indicates the good fit between measured and calculated oscillator strengths (see Table 1) as well as the accuracy of J–O intensity parameters (Ω_λ). Table 2 gives the comparison of J–O intensity parameters in various glass matrices. From the magnitudes of Ω_λ values, one can conclude that the trends of the intensity parameters mainly depend on the ligand environment around the rare-earth ion. According to Jorgensen and Reisfeld [20], the magnitude of the Ω_2 parameter depends on the covalence of metal–ligand bond and also on the asymmetry of ion sites in the neighborhood of rare-earth ion while the magnitudes of Ω_4 and Ω_6 parameters are related to the rigidity of the medium in which the ions are situated. The evaluated Ω_2 parameter for LTTDy10 glass is in good agreement with those obtained for tellurite [21,22] and lead borate [7,23] glasses. Due to the inhomogenity of host around the rare-earth ions, certain absorption band intensities of each rare-earth ions are found to be very sensitive to the ligand environment. These transitions obey the selection rules $\Delta S = 0$, $|\Delta L| \leq 2$, $|\Delta J| \leq 2$ and are known as hypersensitive transitions [24]. The hypersensitive transitions are associated with large values of the reduced matrix elements $\langle \|U^2\| \rangle$ and hence the hypersensitivity is mainly described by the magnitude of Ω_2 intensity parameter [17]. The relative variation of Ω_2 parameter of a rare-earth ion in different environments gives the measure of degree of hypersensitivity exhibited by that ion. In case of Dy^{3+} ion, the $^6H_{15/2} \rightarrow {}^6F_{11/2}$ transition is the hypersensitive transition. In general, the intensity of the hypersensitive transition is higher when compared to the other transitions in any host medium. From Table 1, one can notice that the $^6H_{15/2} \rightarrow {}^6F_{11/2}$ hypersensitive transition in LTTDy10 glass posses higher magnitude of f_{meas} value.

4.3. Excitation and photoluminescence spectra

In order to analyze the luminescence properties as a function of activator (Dy^{3+}) concentration, it is necessary to know the correct excitation wavelength of the ion. For this purpose, the excitation spectrum recorded for LTTDy10 glass by monitoring the emission at 576 nm is shown in Fig. 3. Totally six excitation bands are observed at 352, 365, 388, 426, 452 and 472 nm corresponding to the $^6H_{15/2} \rightarrow {}^5P_{7/2}$, $^5P_{9/2}$, $^4F_{7/2}$, $^4G_{11/2}$, $^4I_{15/2}$ and $^4F_{9/2}$ transitions, respectively. The two excitation bands corresponding to $^6H_{15/2} \rightarrow {}^4I_{15/2}$ and $^6H_{15/2} \rightarrow {}^4F_{9/2}$ transitions are not well resolved due to the small energy gap of ~938 cm^{-1} between the $^4I_{15/2}$ and $^4F_{9/2}$ levels. Since the excitation band corresponding to the $^6H_{15/2} \rightarrow {}^4I_{15/2}$ (452 nm) transition is more prominent, and hence all the LTT glasses have been excited with 452 nm to record the photoluminescence spectra.

Fig. 4 shows the photoluminescence spectra of LTTDy01, LTTDy05, LTTDy10 and LTTDy20 glasses. The spectra contain two relatively intense emission bands: $^4F_{9/2} \rightarrow {}^6H_{15/2}$ (484 nm), $^4F_{9/2} \rightarrow {}^6H_{13/2}$ (576 nm) and two considerably feeble bands: $^4F_{9/2} \rightarrow {}^6H_{11/2}$ (665 nm), $^4F_{9/2} \rightarrow {}^6H_{9/2}$ (750 nm) transitions. The

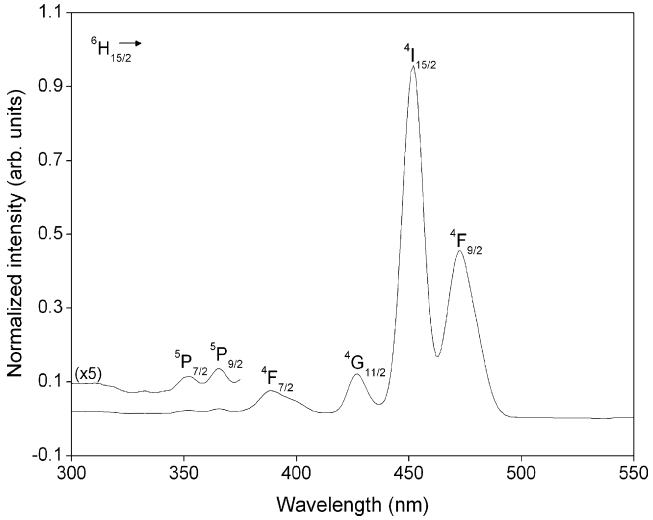

Fig. 3. Excitation spectrum of LTTDy10 glass (λ_{em} = 576 nm).

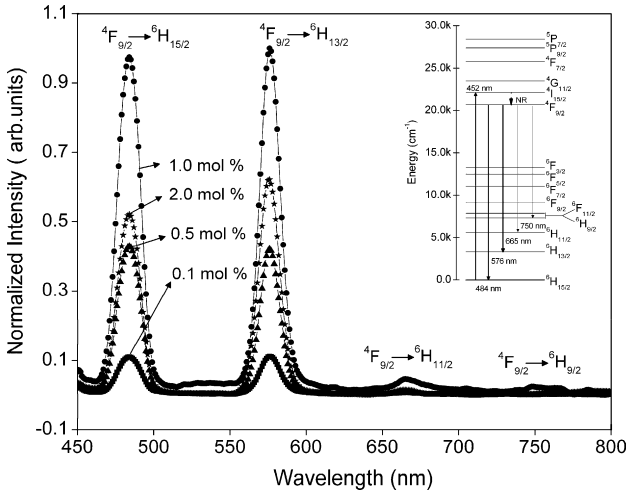

Fig. 4. Photoluminescence spectra for different concentrations of Dy^{3+} ions in LTT glasses. Inset figure shows the partial energy level diagram.

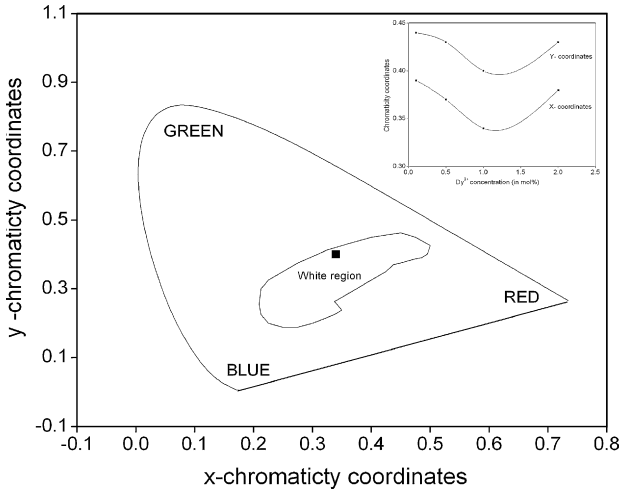

Fig. 6. CIE 1931 chromaticity diagram for LTTDy glasses. Inset shows the variation of color coordinates with Dy^{3+} ion concentration.

$^4F_{9/2} \rightarrow {}^6H_{13/2}$ transition identified in the yellow region is a hypersensitive transition obeying the selection rules $\Delta J = \pm 2$ and $\Delta L = \pm 2$ [24]. Thus, the intensity of this transition is strongly influenced by the surrounding environment. The inset of Fig. 4 illustrates the emission channels of Dy^{3+} ions in LTT glass system. The 452 nm excitation wavelength excites the Dy^{3+} ions to the $^4I_{15/2}$ level. Owing to small energy gap between the $^4I_{15/2}$ and $^4F_{9/2}$ states, the excited Dy^{3+} ions populate the $^4F_{9/2}$ meta-stable state through fast non-radiative decay process. From the $^4F_{9/2}$ excited state to its lower lying $^6H_{J'}$ (J' = 15/2, 13/2, 11/2 and 9/2) states, the radiative transitions occur by the emission of radiations at 484, 576, 665 and 750 nm. With 452 nm excitation the emission of radiation from the LTTDy glasses appears as yellowish-white. This may be mainly due to the large yellow to blue (Y/B) intensity ratio. In the present investigation, the Y/B ratios are found to be 0.92, 1.00, 1.02 and 1.21 for LTTDy01, LTTDy05, LTTDy10 and LTTDy20 glasses, respectively. Fig. 5 represents the variation of Y/B ratio (dotted line) against Dy^{3+} ions concentration.

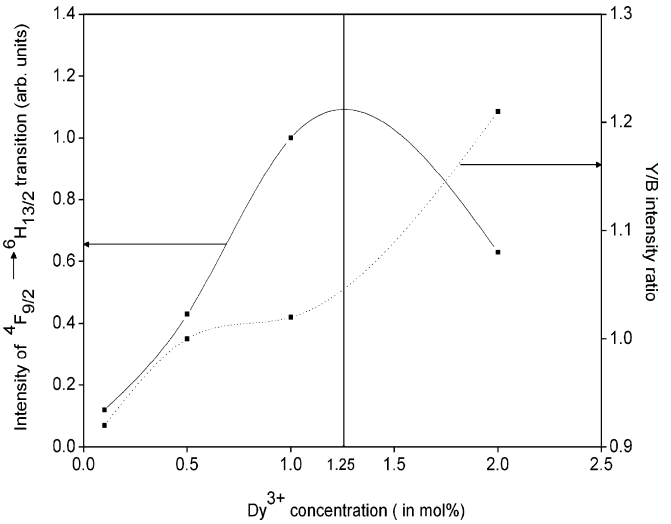

Fig. 5. Variation of fluorescence intensity of $^4F_{9/2} \rightarrow {}^6H_{13/2}$ transition (solid line) and Y/B intensity ratio (dotted line) with Dy^{3+} ion concentration in LTT glasses.

4.4. Luminescence quenching and Dy–O bond covalence

To obtain intense luminescence from an activator ion in any host medium, its concentration should be optimized. In order to optimize the Dy^{3+} ion concentration in LTT glass host, the photoluminescence spectra recorded for LTTDy01, LTTDy05, LTTDy10 and LTTDy20 glasses are shown in Fig. 4. The luminescence intensity increases with increase of Dy^{3+}ions concentration from 0.1 to 1.0 mol%, however the decrease in luminescence intensity has been observed for 2.0 mol%, due to the increasing interaction among the Dy^{3+} ions at higher concentrations. The variation of luminescence intensity of $^4F_{9/2} \rightarrow {}^6H_{13/2}$ transition with Dy^{3+} ion concentration is also shown (solid line) in Fig. 5. This graph shows that the luminescence intensity of Dy^{3+} ions in LTT glass host is higher at 1.25 mol% concentration. From this result one can suggest that the LTT glasses doped with 1.25 mol% of Dy^{3+} ions can generate intense luminescence at 452 nm excitation. In order to know the degree of covalence of Dy–O bond, the variation of yellow to blue (Y/B) intensity ratio of $^4F_{9/2} \rightarrow {}^6H_{13/2}$ and $^4F_{9/2} \rightarrow {}^6H_{15/2}$ transitions for different Dy^{3+} ion concentrations has been plotted as a function of Dy^{3+} ion concentration. The higher Y/B intensity ratios indicate the higher degree of covalence between dysprosium and oxygen ions [23]. The evaluated Y/B intensity ratios reveal that Dy–O covalence increases with increase of Dy^{3+} ion concentration in LTT glasses

4.5. White light emission

Appropriate combinations of blue (B) and yellow (Y) emissions produce white light in addition to the generation and control of different colors in solid state displaying devices [25–27]. The generation of white light by LTTDy glasses has been analyzed in the frame work of the chromaticity color coordinates. In the present investigation, the evaluated color coordinates are (0.39, 0.44); (0.37, 0.43); (0.34, 0.40) and (0.38, 0.43) for LTTDy01, LTTDy05, LTTDy10 and LTTDy20 glasses, respectively. All these coordinates lie within the white light region of in CIE 1931 chromaticity diagram as shown in Fig. 6. For all the concentrations, the deviation in the coordinates is very small as depicted in the inset of Fig. 6.

4.6. Radiative properties

The J–O intensity parameters (Ω_λ) obtained for LTTDy10 glass have been used to estimate certain radiative parameters by using Eqs. (3)–(6), in order to predict the efficient luminescence

Table 3
Different radiative parameters for $^4F_{9/2} \rightarrow {}^6H_{13/2}$ and $^4F_{9/2} \rightarrow {}^6H_{15/2}$ transitions of Dy^{3+} ions in different glasses.

Glass host	λ_P (nm)	$\Delta\lambda_P$ (nm)	A_R (s^{-1})	β_R	β_{mea}	σ_e ($\times 10^{-22}$ cm^2)	$\sigma_e \times \tau_R$ ($\times 10^{-25}$ cm^2)
$^4F_{9/2} \rightarrow {}^6H_{13/2}$ (yellow)							
LTTDy10 [This work]	576	15.91	1730	0.64	0.48	31.20	11.58
Tellurite [28]	576	13.20	319	0.55	–	0.86	–
Leadborate [23]	574	14	1046	0.67	–	–	–
LiTFP [21]	574	–	639	0.66	0.54	27.70	–
NaTFP [21]	574	–	518	0.64	0.54	22.30	–
KTFP [21]	574	–	573	0.64	0.55	24.80	–
LBTAF [7]	576	15.69	714	0.65	0.44	26.13	–
BFB [29]	573	15	734	0.64	–	2.74	–
$^4F_{9/2} \rightarrow {}^6H_{15/2}$ (blue)							
LTTDy10 [This work]	484	17.50	349	0.13	0.51	2.87	1.06
Tellurite [28]	482	15.10	84	0.33	–	0.57	–
Leadborate [23]	479	18	311	0.20	–	–	–
LiTFP [21]	483	–	98	0.10	0.44	1.70	–
NaTFP [21]	483	–	91	0.11	0.45	1.60	–
KTFP [21]	483	–	108	0.12	0.43	1.80	–
LBTAF [7]	484	17.60	161	0.15	0.55	2.62	–
BFB [29]	481	17	194	0.19	–	0.32	–

characteristics of two intense $^4F_{9/2} \rightarrow {}^6H_{13/2}$ and $^4F_{9/2} \rightarrow {}^6H_{15/2}$ transitions. The evaluated radiative transition probabilities (A_R), fluorescence branching ratios (β_R), stimulated emission cross-sections (σ_e) and optical gain parameters ($\sigma_e \times \tau_R$) presented in Table 3 are found to be in good agreement with those reported in literature [7,21,23,28,29].

The branching ratios and stimulated emission cross-sections are the important laser parameters which predict the luminescence efficiency of host material. In the present study, it could be observed that, the values of branching ratio (β_R) and stimulated emission cross-section (σ_e) for the $^4F_{9/2} \rightarrow {}^6H_{13/2}$ transition are found to be maximum among all the other transitions. The higher magnitudes of branching ratio and stimulated emission cross-section of $^4F_{9/2} \rightarrow {}^6H_{13/2}$ transition suggest the suitability to accomplish laser action in LTTDy10 glass. The optical gain parameter ($\sigma_e \times \tau_R$), which is the measure of laser threshold, is also larger than that of barium fluoroborate glass [29].

4.7. Fluorescence decay analysis

Fig. 7 shows the decay curves of $^4F_{9/2}$ excited state for various Dy^{3+} ion concentrations. For all the Dy^{3+} concentrations, the decay curves show single-exponential nature. The measured lifetimes (τ_{meas}) obtained by taking the first e-folding times of the decay curves are 248, 226, 152 and 146 μs for LTTDy01, LTTDy05, LTTDy10 and LTTDy20 glasses, respectively. The decrease of τ_{meas} values with the increase of Dy^{3+} concentration is mainly due to the increasing interaction among the Dy^{3+} ions at higher concentrations. The inset of Fig. 7 shows the variation of τ_{meas} values with Dy^{3+} concentration. The measured lifetime (152 μs) of $^4F_{9/2}$ level of LTTDy10 glass is found higher than those reported for borate (140 μs) [30], phosphate (100 μs) [30] and fluorozirconate (120 μs) [31] glasses.

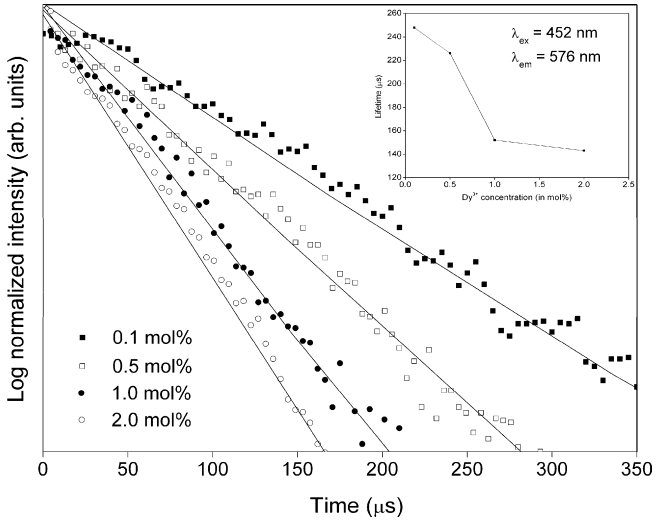

Fig. 7. Decay curves of $^4F_{9/2}$ excited state of Dy^{3+} ion in LTT glasses. Inset depicts the variation of lifetimes of $^4F_{9/2}$ level with Dy^{3+} ion concentration.

The predicted radiative lifetime (τ_R) of $^4F_{9/2}$ excited level obtained from J–O theory [17,18] is 377 μs. The considerable difference between the magnitudes of τ_R and τ_{meas} values of $^4F_{9/2}$ level indicates that the emission from this level is not fully radiative but there should also be some non-radiative decay contributions. In general, the non-radiative contribution might take place due to either energy transfer among the Dy^{3+} ions or multiphonon relaxation or both. In the present Dy^{3+}-doped LTT glass system the decrease in measured lifetimes could be due to the role of energy transfer among the Dy^{3+} ions at higher concentrations.

5. Conclusions

The room temperature absorption and photoluminescence spectra of Dy^{3+}-doped in LTT glasses were recorded and analyzed using the Judd–Ofelt theory. Reasonably small δ_{rms} of $\pm 0.34 \times 10^{-6}$ obtained between the measured and calculated oscillator strengths indicates the accuracy of J–O intensity parameters. The luminescence quenching of the emission transitions originating from the $^4F_{9/2}$ excited state to its lower lying states with increase of Dy^{3+} concentration has been discussed. From the Y/B luminescence intensity ratios, it is suggested that the Dy–O covalence increases with increase of Dy^{3+} ion concentration. The color coordinates evaluated for appropriate combinations of yellow to blue emissions can be made to match with those of white light region of CIE chromaticity diagram. The higher values of branching ratios and stimulated emission cross-sections for the $^4F_{9/2} \rightarrow {}^6H_{13/2}$ transition suggest the utility of LTTDy10 glass as potential laser material. For all the Dy^{3+} concentrations, the fluorescence decay curves show single-exponential nature. The variation of $^4F_{9/2}$ excited level lifetimes with Dy^{3+} concentration has been attributed to the increasing interaction among the Dy^{3+} ions at higher concentrations. The present investigations suggest that the LTT glasses doped with 1.25 mol% of Dy^{3+} ions could be useful for potential laser material as well as to generate white light in color displaying devices.

Acknowledgements

One of the authors Prof. L.R. Moorthy would like to thank Defence Research and Development Organization (DRDO), New Delhi for the sanction of financial support in the form of major research projects No.ERIP/ER/0603593/M/01/984. Mr. A. Mohan Babu is also thankful to the DRDO for the financial support through Project Assistant in the above project.

References

[1] L. Xiao, Q. Xiao, Y. Liu, P. Ai, Y. Li, H. Wang, J. Alloys Compd. 495 (2010) 72–75.
[2] J. Pisarska, R. Lisecki, W. Ryba-Romanowski, T. Goryczka, W.A. Pisarski, Chem. Phys. Lett. 489 (2010) 198–201.
[3] J. Suresh Kumar, K. Pavani, A. Mohan Babu, N.K. Giri, S.B. Rai, L. Rama Moorthy, J. Lumin. 130 (2010) 1916–1923.
[4] W.A. Pisarski, J. Pisarska, G. Dominiak-Dzik, W. Ryba-Romanowski, J. Alloys Compd. 484 (2009) 45–49.
[5] G. Lakshminarayana, J. Qiu, J. Alloys Compd. 476 (2009) 470–476.
[6] Y. Dwivedi, S.B. Rai, Opt. Mater. 31 (2009) 1472–1477.
[7] B.C. Jamalaiah, J. Suresh Kumar, T. Suhasini, K.W. Jang, H.S. Lee, H.J. Choi, L. Rama Moorthy, J. Alloys Compd. 474 (2009) 382–387.
[8] C. Basava Poornima, C.K. Jayasankar, P.P. Chandrachoodan, Physica B 404 (2009) 235–242.
[9] M. Jayasimhadri, K.W. Jang, H.S. Lee, B. Chen, S.S. Yi, J.H. Jeong, J. Appl. Phys. 106 (2009), 013105-4.
[10] Z. Yang, B. Li, F. He, L. Luo, W. Chen, J. Non-Cryst. Solids 354 (2008) 1198–1200.
[11] H. Lin, E.Y.B. Pun, X. Wang, X. Liu, J. Alloys Compd. 390 (2005) 197–201.
[12] R.A.H. El-Mallawany, Tellurite Glasses Handbook-Physical Properties and Data, CRC, Boca Raton, FL, 2001.
[13] G. Poirier, F.S. Ottoboni, F.C. Cassanjes, A. Remonte, Y. Messaddeq, S.J.L. Ribeiro, J. Phys. Chem. B 112 (2008) 4481–4487.
[14] M. Ohtsuki, R. Tamura, S. Takeuchi, S. Yoda, T. Ohmura, Appl. Phys. Lett. 84 (2004) 4911–4913.
[15] M.A. Engelhardt, S.S. Jaswal, D.J. Sellmyer, Phys. Rev. B 44 (1991) 12671–12679.
[16] C. Görller-Walrand, K. Binnemanns, in: K.A. Gschneidner Jr., L. Eyring (Eds.), Handbook on the Physics and Chemistry of Rare Earths, North-Holland, Amsterdam, 1998, pp. 101–264.
[17] B.R. Judd, Phys. Rev. B 127 (1962) 750–761.
[18] G.S. Ofelt, J. Chem. Phys. 37 (1962) 511–520.
[19] W.T. Carnall, P.R. Fields, K. Rajak, J. Chem. Phys. 49 (1968) 4424–4442.
[20] C.K. Jorgensen, R. Reisfeld, J. Less-Common Met. 93 (1983) 107–112.
[21] M. Jayasimhadri, L.R. Moorthy, K. Kojima, K. Yamamoto, N. Wada, N. Wada, J. Phys. D: Appl. Phys. 39 (2006) 635–641.
[22] J. Hormadely, R. Reisfeld, J. Non-Cryst. Solids 30 (1979) 337–348.
[23] J. Pisarska, J. Phys.: Condens. Matter 21 (2009) 285101.
[24] S. Tanabe, T. Ohyagi, N. Soga, T. Hanada, Phys. Rev. B 46 (1992) 3305–3310.
[25] L.A. Diaz-Torres, E. De La Rosa, P. Salas, V.H. Romero, C. Angeles-Chavez, J. Solid State Chem. 181 (2008) 75–80.
[26] J. Kuang, Y. Liu, J. Zhang, J. Solid State Chem. 179 (2006) 266–269.
[27] V. Lavin, F. Lahoz, I.R. Martin, U.R. Rodriguez-Mendoza, in: R. Balda (Ed.), Photonic Glasses, Research Signpost, Trivandrum, India, 2006, pp. 115–149.
[28] V.K. Rai, S.B. Rai, D.K. Rai, Opt. Commun. 257 (2006) 112–119.
[29] Y. Dwivedi, S.B. Rai, Opt Mater. 31 (2009) 1472–1477.
[30] G.S. Raghuvanshi, H.D. Bist, H.C. Khandpal, J. Phys. Chem. Solids 43 (1982) 781–783.
[31] V.M. Orera, P.J. Alonso, R. Cases, R. Alcala, Phys. Chem. Glasses 29 (1988) 59–62.